1. Publication NQ INPE-3647-RPE/484	2. Version	3. Date Sept., 1985	5. Distribution ☐ Internal ☒ External ☐ Restricted
4. Origin DME/DPM-DAM	Program PNTE		

6. Key words - selected by the author(s)

MODELO NUMÉRICO
PARAMETRIZAÇÃO
FLUXO RADIATIVO

7. U.D.C.: 551.511.61

8. Title INPE-3647-RPE/484 RADIATIVE FLUX PARAMETERIZATIONS IN A BOUNDARY LAYER MODEL	10. NQ of pages: 36
	11. Last page: 29
	12. Revised by *Yoshihiro Yamazaki*
9. Authorship Sergio Henrique Franchito Nelson Arai José Paulo Bonatti Responsible author	13. Authorized by *Marco Antonio Raupp* *Director General*

14. Abstract/Notes

A software for atmospheric radiative heating and cooling using the parameterization of Kuo and Qian was developed. This parameterization was introduced in a simple planetary boundary layer model, substituting the Brunt's and Chang's parameterization for long and short wave radiation respectively in the first version of the model. Experiments using both parameterizations were made and the results seem to be in a good agreement with real data.

15. Remarks

ACKNOWLEDGMENTS

CONTENTS

LIST OF FIGURES

1. INTRODUCTION

The evaporation of water and the exchange of water vapour heat and momentum between the atmosphere and the land/ocean surface are among other processes mechanisms of paramount importance in the planetary boundary layer (PBL).

Momentum transfer by viscous forces supplies the turbulent kinectic energy (KE) source and creates vertical wind shear. Radiative fluxes toward or from surface gives or removes sensible heat to or from atmosphere, generating temperature differences between air and Earth surface. Then, the fluctuation forces act as KE source when heat flux is from surface, making unstable the PBL. When the flux is toward the surface the fluctuation forces act as sinks of KE, inhibiting the turbulence and making stable the PBL. The surface evaporation also generates fluctuation forces which are KE sources. These fluxes are very important for the dynamic of the atmosphere in meso and large scale, because they are the principal sources of atmospheric motions.

As pointed by Smith and Carson (1977) the internal structure of PBL in numerical models over land must be determined by surface fluxes and external parameters.

In despite of their simplicity, unidimensional models present some essential and common aspects with bi and three-dimensional models.

In this work, the parameterization of Kuo and Qian (1981) for radiative heating and cooling is introduced in a simple model for planetary boundary layer (Franchito and Yamazaki, 1982). This was made substituting the Brunt's (1952) and Chang's (1979) parameterization for long and short wave radiation, respectively, in the model.

2. PLANETARY BOUNDARY LAYER MODEL

The prognostic equations for the planetary boundary layer were only considered in one dimension. Nevertheless, the inclusion of horizontal advective effects could extend the model for two or three dimensions. The relevant equations of the present formulation are:

$$\frac{\partial u}{\partial t} = f(v - v_g) + \left(\frac{\delta u}{\delta t}\right)_m , \tag{1}$$

$$\frac{\partial v}{\partial t} = -f(u - u_g) + \left(\frac{\delta v}{\delta t}\right)_m , \tag{2}$$

$$\frac{\partial \theta}{\partial t} = \left(\frac{\delta \theta}{\delta t}\right)_m , \tag{3}$$

where:

u   ... wind speed relative to Earth in x direction,

u_g ... geostrophic wind speed in x direction,

t   ... time,

f   ... Coriolis parameter,

v   ... wind speed relative to Earth in y direction,

v_g ... geostrophic wind speed in y direction,

θ   ... potential temperature of air.

The terms with subscript "m", for the levels above the surface layer, are related with the Richardson's number adjustment scheme as proposed by Chang (1979); and   for the surface layer it will be adopted the Blackadar's (1976) formulation. Following the above two authors the prognostic equation for the earth's surface can be represented by:

$$\frac{\partial T_g}{\partial t} = (I_S\!\downarrow + I_L\!\downarrow \div I_L\!\uparrow)\ C_g^{-1} + RTC(T_m - T_g) + K_S(\theta_a - T_g)\ , \qquad (4)$$

where the effects of insolation absorbed by surface, atmospheric long wave radiation, surface long wave radiation, heat exchange between the surface layer and the substract, and surface heat flux are included.

In this equation:

T_g ... ground temperature,

$I_S\!\downarrow$... downward short wave flux,

$I_L\!\downarrow$... downward long wave flux,

$I_L\!\uparrow$... upward long wave flux,

C_g ... heat capacity per unit area of slab,

RTC... relaxation time constant,

K_S ... thermal diffusivity of soil,

θ_a ... screen level potential temperature,

T_m ... air surface temperature (usually the average of the previous 24 h).

3. RADIATIVE HEATING AND COOLING

3.1 - CHANG's AND BRUNT's PARAMETERIZATION

As suggested by Chang (1979) the short wave radiation absorbed by surface can be written as:

$$I_S\downarrow = S \cos Z\ (1-A)\ q^{\sec Z}, \qquad (5)$$

where:

S ... solar constant,

Z ... zenith angle of the sun,

A ... surface albedo,

q ... atmospheric transmissivity.

The zenith angle of the sun is obtained using:

$$Z = \cos^{-1}\ (\sin \psi \sin \delta + \cos \psi \sin \delta \cos h)\ , \qquad (6)$$

where

$$\delta = 23.5\ \sin \left[\frac{2\pi(D-80)}{365} \right],$$

$$h = 15^o\ (LT - 12^o)\ ,$$

$$LT = t - \frac{\lambda}{15^o}$$

here:

ψ ... latitude,

δ ... declination of the sun,

h ... hour angle of the sun,

D ... day of year,

λ ... longitude,

t ... Greenwich mean Time.

The long wave radiation as proposed by Brunt (1952) is given by:

$$I_L\downarrow - I_L\uparrow = - \varepsilon\sigma \, T_g^4 \, (1\text{-}a\text{-}b \sqrt{e}) \, , \tag{7}$$

where a and b are constants. In this formulation the water vapor effect was neglected (b=0) and a was taken as 0.61.

3.2 - KUO AND QIAN (1981) PARAMETERIZATION

3.2.1 - SOLAR RADIATION

The entire solar energy spectrum is affected differently by the atmospheric constituents. Then it is convenient to divide the solar spectrum into bands with respective attenuating physical process proper to each one. One common separation is to take the ultraviolet ($\lambda < 0.3\mu m$), visible ($0.3 < \lambda < 0.7\mu m$) and infrared ($\lambda > 0.7\mu m$) separately as suggested by Kuo and Qian (1981). The energy content of these three regions are 1.296, 47.834 and 50.870% of the total solar energy flux ($S_0 = 1372 \, W \, m^{-2}$),respectively.

Because the quantity of solar energy,which reaches the ground, in the $\lambda < 0.3\mu m$ region is low, it will be neglected in this work. To study the attenuation of solar radiation in 0.3 - 0.7 μm region, Kuo and Qian (1981) integrated the scattering transmissivity function $\tau_S(\lambda)$ given by Kondratyev (1969) and obtained an empirical formula for albedo a_0^* of clear sky atmosphere, in this spectral range, using optical path lenght of atmosphere:

$$a_o^* = 0.0483m - 0.0088m^2 \text{ for } 0 \leqslant m \leqslant 1 \text{ ,} \tag{8}$$

$$a_o^* = 0.0086 + 0.0328m - 0.0020m^2 \text{ for } 1 \leqslant m \leqslant 16 \text{ ,} \tag{9}$$

where:

$$m = \left[\frac{p \text{.sec } Z}{1.000} \right] \text{ .}$$

The main physical process that attenuates the solar radiation in this band is the scattering. Then, the solar energy flux in this band is given by:

$$S^{(2)} = 0.478345 S_0 \cos Z \text{ ,} \tag{10}$$

or in terms of reflection coefficient:

$$a_o = \frac{a_o^*}{0.478345} \text{ .} \tag{11}$$

The amount of energy that reaches the surface is $(1-a_{os}) \, S^{(2)}$, where a_{os} is the value of a_o at surface. Considering the influence of multiple scattering by the surface and atmosphere, the solar energy absorbed by the surface in this region is given by:

$$S_g^{(2)} = S^{(2)} \cdot \frac{(1-a_{os}) \, (1-a_s)}{(1-a_{os} \, a_s)} \text{ ,} \tag{12}$$

where a_s is the surface albedo.

The combined cloud albedo (R_c) and above cloud atmosphere is given as:

$$a_c = a_o + (1-a_o) \, R_c \text{ .} \tag{13}$$

To simplify the methodology, the assumptions of no absorption of solar energy in this region by clouds and the cloud albedo (R_c) of 0.50 are made. Then, the solar energy absorbed by surface in cloudy atmosphere is given by:

$$S_g^{(2)} = S^{(2)} \frac{(1-a_c)\ (1-a_s)}{(1-a_c\ a_s)} \ , \qquad (14)$$

and

$$a_c = a_0 + (1-a_0)\ 0.5$$

In the region of $\lambda > 0.7\mu m$ the attenuation is mainly due to absorption and scattering by water vapor. The water vapor absorption can be calculated using:

$$\Delta S^{(3)} = B.\omega^{0.303} \ , \qquad (15)$$

here

B = 0.186, $\omega = m_\omega$ sec Z, ω is the effective water vapor path lenght and m_ω is the water vapor content of the atmosphere in the layer.

If cloud is present, then the absorption of solar radiation in the layers below the cloud top must be computed diferently to allow for the influence of reflection by the cloud and the fact that the solar radiation will become diffuse below the cloud top. Then, the intensity of the solar radiation in this spectral range at the cloud top is given by:

$$S_t^{(3)} = S_0^{(3)} - \Delta S_t^{(3)} \ , \qquad (16)$$

where $\Delta S_t^{(3)}$ is the value of $\Delta S^{(3)}$ for $\omega_t = m_{zt}$ sec Z, and m_{zt} is the water vapor content of the air column above the cloud. It is assumed that there is no further absorption of the solar radiation reflected by the cloud.

Then, the amount of solar energy reflected by the cloud to space in this spectral range is a $R_c S_t^{(3)}$. Effective reflectivity can be defined as:

$$R_c^* = \frac{1}{S_0^{(3)}} a R_c S_t^{(3)} = a R_c \left(1 - \frac{\Delta S_t^{(3)}}{S_0^{(3)}}\right) , \qquad (17)$$

where a is the fraction of cloud cover.

The effective downward-radiated solar energy in this spectral range at the top of the atmosphere can be defined by:

$$S_{eo}^{(3)} = (1-R_c^*) S_0^{(3)} = (1-a R_c) S_0^{(3)} + a R_c \Delta S_t^{(3)} . \qquad (18)$$

The total water vapor path length at height Z below the cloud top, Z_t, is the sum of the direct path lenght above and the diffuse path length below the cloud top:

$$\omega_e = m_{zt} \sec Z + 1.6667 \Delta m_z , \qquad (19)$$

where Δm_z is the water vapor content between Z and Z_t.

The absorption of solar energy in this spectral range from the top of the atmosphere to the level Z is given by:

$$\Delta S^{(3)} = \frac{B}{S_0^{(3)}} S_{eo}^{(3)} \omega_e^{0.303} . \qquad (20)$$

The solar energy absorbed at any layer can then be calculated. The part of $S_{eo}^{(3)}$ which reaches the earth's surface is:

$$S_{es}^{(3)} = S_{eo}^{(3)} - \Delta S^{(3)} = S_{eo}^{(3)} \left[1 - \frac{B}{S_0^{(3)}} \omega_{es}^{0.303}\right] , \qquad (21)$$

where ω_{es} is the effective total water vapor path length at the surface. The part $a_s \, S_{es}^{(3)}$, reflected by the surface to space, constitutes part of the earth's albedo,while the other is absorbed by the surface and is given by:

$$\Delta S_g^{(3)} = (1-a_s) \; S_{eo}^{(3)} \left[1 - \frac{B}{S_o^{(3)}} \, \omega_{es}^{0.303} \right] .$$

(22)

3.2.2 - TERRESTRIAL LONG WAVE RADIATION

Terrestrial infrared radiation acting in the layer Z to Z + ΔZ produces a heating rate given by:

$$HR = \frac{\left[G(Z+\Delta Z) - G(Z) - F(Z+\Delta Z) + F(Z)\right]}{\Delta Z} ,$$

(23)

where F and G are the upward and downward fluxes of long wave radiation, respectively. As made by Kuo (1977), the long wave radiation spectrum is divided into four intervals and a representative mean transmission function τ_j is used for the spectral interval $\Delta \gamma_j$ to calculate the infrared heating rate in that interval. The relationship $\tau_j(u+\Delta u) = \tau_j(u) \cdot \tau_j(\Delta u,u)$ and mean value theory are used to evaluate the emissivity of the layer (Z, Z+ΔZ). Here, u is the optical thickness of the layer.

Then:

$$F_j(Z+\Delta Z) = F_j(Z) \; \tau_j(\Delta u,u) + \bar{B}_j \left[1 - \tau_j(\Delta u,u)\right] ,$$

(24)

$$G_j(Z) = G_j(Z+\Delta Z) \; \tau_j(\Delta u,u) + \bar{B}_j \left[1-\tau_j(\Delta u,u)\right] ,$$

(25)

$$HR_j = \left\{G_j(Z+\Delta Z) + F_j(Z) - 2\bar{B}_j(Z)\right\} \frac{\left[1-\tau_j(\Delta u,u)\right]}{\Delta Z} ,$$

(26)

where $\overline{B}_j$ is the mean blackbody emissivity and $\tau_j(\Delta u, u)$ is the slab transmissivity of the layer.

One can calculate HR_j from layer to layer consecutively if it is assumed that $F_j(0) = \sigma\, T_s^4$ and $G_j(\infty) = 0$. The transmission function, $T_j(\Delta u)$, depends upon u and should be calculated from:

$$T_j(\Delta u, u) = \frac{T_j(u + \Delta u)}{\tau_j(u)} , \qquad (27)$$

for the finite spectral interval $\Delta \nu_j$.

In the interval 0-500cm^{-1} band the mean water vapor transmissivity $\tau_1^{(\omega)}$ is given by:

$$\tau_1^{(\omega)} = 0.20001\ E_1(Y_{1l}) - 0.39999\ E_1(Y_{1h}) + 0.199998\ E_1(Y_{2h}). \qquad (28)$$

Functions used in the above equation are defined by:

$$E_1(u) = \int_u^\infty u^{-1}\ e^{-u}\ du ,$$

$$Y_{1h} = \frac{56.234\ m_q}{\sqrt{m_q + 0.0001}} , \qquad Y_{1l} = Y_{1h} \cdot e^{-1.675},$$

$$Y_{2h} \sim Y_{1l}$$

here m_q is the effective absorbing mass of water vapor of the layer. $E_1(u)$ is calculated with a polynomial approximation for $0 \leq u \leq 1$ and a rational approximation for $1 < u = \infty$. These approximations are given in Kuo (1977).

The transmissivities τ_2, τ_3 and τ_4 are for the spectral intervals $500\text{-}800\text{cm}^{-1}$, $800\text{-}1250\text{cm}^{-1}$ and $1250\text{-}2250\text{cm}^{-1}$, respectively. Then:

$$\tau_2 = (\tau_2^{(\omega)}) \cdot (\tau_2^{(c)}) \; . \tag{29}$$

The water vapor and carbon dioxide transmissivities are defined by:

$$\tau_2^{(\omega)} = \frac{1}{3} \left[E_1(Y_{31}) - E_1(Y_{3h}) \right] , \tag{30}$$

$$\tau_2^{(c)} = \frac{1}{3} \left\{ 0.4 \left[E_1(\eta) - E_1(518\eta) \right] + 0.053 \left[E_1(Z') - E_1(Z_0') \right] \right\} , \tag{31}$$

and

$$Y_{3h} = Y_{1h} \, e^{-3.3235}, \quad Y_{31} = Y_{3h} \cdot e^{-3.0},$$

$$Z = 1.5 \times 10^{-6} \, m_c \, , \quad Z_0 = 12582Z \, ,$$

$$\eta = \frac{0.0041 m_c}{\sqrt{m_c}} \, ,$$

where m_c is the effective absorbing mass of carbon dioxide at normal pressure and temperature.

The transmissivity for the third spectral interval, τ_3, is given by:

$$\tau_3 = 0.6441 \left\{ E_1(Y_{41}) - E_1(Y_{4h}) \right\} , \tag{31}$$

here

$$Y_{4h} = \frac{0.5427m_q}{\sqrt{1+4m_q}} \; , \quad Y_{41} = 0.2117 \; Y_{4h} \; .$$

For τ_4:

$$\tau_4 = 0.2506 \left\{ E_1(0.01518Y_{1h}) - E_1(0.2291Y_{1h}) \right\} \; . \tag{32}$$

The blackbody emissivity, $\overline{B}_j(T)$, is calculated from:

$$B_j(T) = A \left\{ G(X_{j-1}) - G(X_j) \right\} \; , \tag{33}$$

where:

$$A = \frac{15}{\pi^4} \; \sigma_{SB} \; T^4 \; ,$$

σ_{SB} = Stefan-Boltzmann constant

$$G(X) = X^3 S_1(X) + 3X^2 \; S_2(X) + 6 \, X \, S_3(X) + 6 \; S_4(X) \; ,$$

$$X = \frac{hC.\nu}{kT} = \frac{1.43880\nu}{T} \; ,$$

$$S_k = \sum_{h=1}^{\infty} \frac{e^{-hX}}{h^k} \quad \text{for } k = 1,2,3,4 \; ,$$

$$G(0) = \frac{\pi^4}{15} \; .$$

4. STABILITY AND MIXING CONDITIONS

The layer that controls the heat flux from surface to the atmosphere was considered as having twice the screen-level height. The heat balance in this layer requires, in the absence of adiabatic heat sources, that the internal energy be modified only by interaction with surface and by transfer to the mixed layer, i.e.

$$\frac{\partial \Theta_a}{\partial t} = \frac{C_g}{\rho c_p d} K_s (T_g - \Theta_a) - \frac{H_o}{\rho c_p d} \quad , \tag{34}$$

where

Θ_a — screen level potencial temperature,

ρ — density,

c_p — specific heat of dry air at constant pressure,

d — two times screen level layer,

T_g — ground temperature,

H_o — total heat flux.

The total heat flux (H_o) is the sum of mechanical (H_m) and convective (H_c) fluxes. The convective flux is calculate using Priestley's aerodynamic method. Under convectively unstable conditions, for heights above Z_m (height where $R_i \sim 0\ 25$), H_c could be estimate by:

$$H_c = \frac{h \rho c_p}{3^{3/2} \left(1 - \frac{Z_A}{Z_N} \right)^{3/2}} \left(\frac{g}{\overline{\Theta}} \right)^{1/2} \cdot Z_A^{1/2} (\Theta_a - \Theta_N)^{3/2} \quad , \tag{35}$$

here:

h - Priestley's constant,

Z_A - screen level height,

Z_N - 50m level,

g - acceleration of gravity,

$\overline{\Theta}$ - mean potential temperature,

Θ_N - potential temperature at Z_N.

The mechanical heat flux generated by vertical wind shear, which acts over vertical temperature gradient near the ground, is the cause only of heat exchange mechanism in nonconvective situations ($\Theta_a \leq \Theta_N$). This flux is calculated using the Monin-Obukhov's similarity theory. The relationships given by Businger (1973) are applied to a method proposed by Hoffert and Storch (1979):

$$H_m = \rho c_p\, u^* \, T^* \, , \tag{36}$$

where:

u^* - friction velocity,

T^* - frictional temperature scale,

$$u^* = \frac{K\, u_a}{\ln\left(\dfrac{Z_a}{Z_0}\right) - \psi_u\left(\dfrac{Z_a}{L}\right)} \, ,$$

$$T^* = \frac{K(T_a - T_g)}{\alpha_0\left[\ln\left(\dfrac{Z_a}{Z_0}\right) - \psi_T\left(\dfrac{Z_a}{L}\right)\right]} \, ,$$

$$L = \frac{\alpha_0 \, u_a \, T_g}{g(T_a - T_g)} \frac{\left[\ln\left(\frac{Z_a}{Z_0}\right) - \psi_T \left(\frac{Z_a}{L}\right) \right]}{\left[\ln\left(\frac{Z_a}{Z_0}\right) - \psi_u \left(\frac{Z_a}{L}\right) \right]^2} \quad,$$

where

ψ_u - stability function for wind,

ψ_T - stability function for temperature,

and

k - Von Kãrmann constant (1.35),

u_a - screen level wind speed in x direction,

Z_0 - aerodynamic roughness lengthscale,

T_a - screen level temperature,

α_0 - a constant equal to 0.74.

In the surface layer, 3m in the present model, the wind direction is supposed constant near the ground as suggested by Blackadar (1976). So that, the stress tensor has the same direction of wind in a given level. The mixing effects in the 50m layer are obtained by:

$$\left(\frac{\partial u_N}{\partial t}\right)_m = - \frac{u^{*2}}{Z_N} \cdot \frac{u_N}{|\mathbf{V}_N|} \quad, \tag{37}$$

$$\left(\frac{\partial v_N}{\partial t}\right)_m = - \frac{u^{*2}}{Z_N} \cdot \frac{v_N}{|\mathbf{V}_N|} \quad, \tag{38}$$

$$\left[\frac{\partial \Theta_N}{\partial t}\right]_m = \frac{\Theta_N}{T_N} \cdot \frac{H_o}{\rho \, c_p \, Z_N} \ , \tag{39}$$

where:

subscript N denotes values at 50m height and **V** is the horizontal velocity vector.

In the layers above 50m the heat and momentum distribution are made using Richardson's number adjustment scheme as suggested by Chang (1979):

$$Ri = \frac{\dfrac{g}{\Theta} \cdot \dfrac{\partial \Theta}{\partial z}}{\left[\left(\dfrac{\partial u}{\partial z}\right)^2 + \left(\dfrac{\partial v}{\partial z}\right)^2\right]} \ . \tag{40}$$

Two important mechanism contribute for occurrence of mixing in layers below the inversion: in convective or near neutral conditions the mixing could be produced by static unstability; while in stable conditions the principal mechanism is the vertical wind shear. Then, when Richardson number between two layers reaches a critical value the mixing between two layers occurs. This critical value was taken as 0.25 as suggested by Taylor (1931), Businger (1969), Hines (1971) and other authors.

An adjustment is made for two layers with different potential temperatures Θ_j and Θ_{j+1} and $Ri < 0.25$, so that the vertical temperature rate (γ_c) is given by:

$$\Theta'_{j+1} - \Theta'_j = \frac{\gamma_c}{g} \left(\phi_{j+1} - \phi_j\right), \tag{41}$$

where Θ'_{j+1} and Θ'_j are the potential temperatures at levels $j+1$ and j after the adjustment, and ϕ_{j+1}, ϕ_j are geopotential at the same levels.

In this model $\gamma_c = 7 \times 10^{-4}$ Km^{-1} as suggested by Deardorff (1966). The new potential temperature at level $j+1$ after the adjustment is obtained considering that potential temperature is preserved during adiabatic mixing:

$$\Theta'_{j+1} = \frac{\left[\Theta_{j+1} \, \delta z_{j+1} + \Theta_j \, \delta z_j + \dfrac{\gamma_c}{g} (\phi_{j+1} - \phi_j) \, \delta z_j \right]}{(\delta z_{j+1} + \delta z_j)} , \qquad (42)$$

where δz_{j+1} e δz_j are the layer's thickness.

The new value of temperature at level j is obtained by equation (41), using Θ'_{j+1} from equation (42). The proportion of mass (α) transferred from the level j to $j+1$ for temperature adjustment is given by:

$$\alpha = \frac{\Theta'_{j+1} - \Theta_j}{\Theta_j - \Theta_{j+1}} . \qquad (43)$$

This value of α is used for momentum adjustment:

$$\mathbf{V}'_{j+1} = (1 - \alpha) \, \mathbf{V}_{j+1} + \alpha \mathbf{V}_j . \qquad (44)$$

The new value of wind velocity at level j is obtained from the momentum conservation:

$$\mathbf{V}'_j = \frac{(\mathbf{V}_{j+1} - \mathbf{V}'_{j+1}) \, \delta z_{j+1} + \mathbf{V}_j \, \delta z_j}{\delta z_j} . \qquad (45)$$

There are no explicit expression for $(\partial u/\partial t)_m, (\partial v/\partial t)_m$ and $(\partial \theta/\partial t)_m$ terms of equations (1)-(3) above the surface layer, because they are implicitly evaluated for all layers by adjustment of equations (41)-(45).

5. RESULTS

Two different parameterizations of radiative transfer were implemented for a PBL model, the first based on Brunt's and Chang's scheme, and the other on Kuo and Qian's method. In both cases, the model was initialized using observed data collected during the "Great Plain Experiment" held on August, 9th, 1953 (Lettau and Davidson, 1957). The initial potential temperature profile, corresponding to that observed at 4:00 h (local time), is presented in Figure 1.
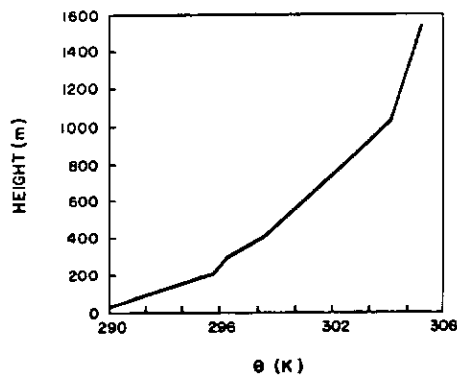
Fig. 1 - Initial potential temperature profile.

The model response to sensitivity test, conducted using different initial temperature profile, revealed that it is not greatly influenced by initial wind because strong mixing process occurs in the morning. So that it was considered reasonable to take wind with approximatly logarithmic profile and u_g, v_g assumed as zero (calm situation).

The dry case was first considered taking Brunt's and Chang's (case A), and Kuo and Qian's (case B) parameterizations without water vapor. The effect of humidity was then investigated taking the Kuo and Qian's parameterization with water vapor (case C) and comparing the results with the case B.

5.1 - COMPARISON BETWEEN CASE A AND CASE B

In both cases the diurnal variation of some relevant parameters of the PBL was well simulated. The main differences appear in the intensities of the incoming radiation flux and in the upward net long wave flux, as presented in Figures 2 and 3, respectively. During the day, short wave flux absorbed in surface is greater in case B, which compensates the amount of energy lost to space that is also greater in case B. So that, the net radiation fluxes are almost the same in both cases, as showed in Figure 4.
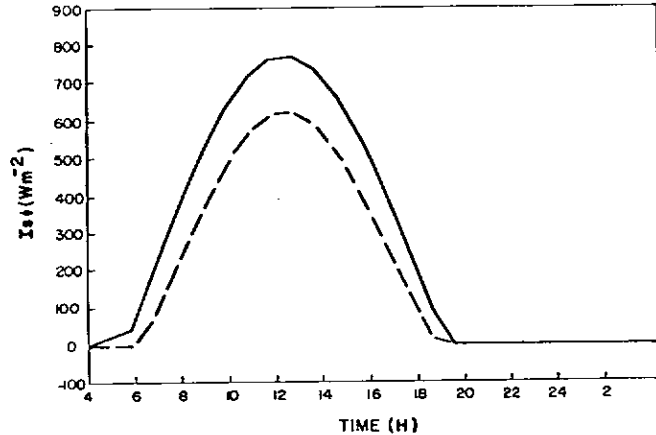
Fig. 2 - Diurnal variation of the solar radiation flux.

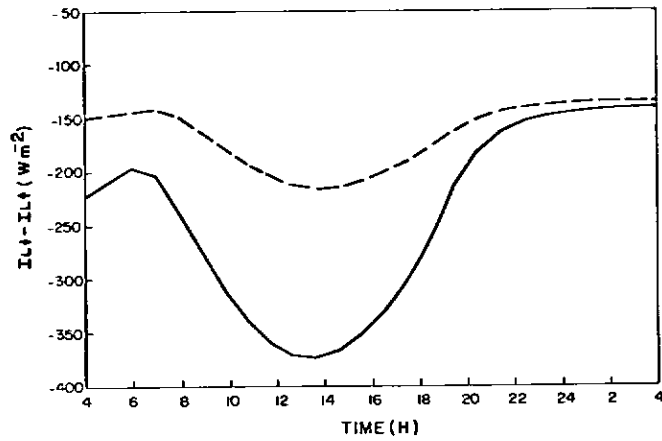Dashed line for case A.

Full line for case B.

Fig. 3.- Diurnal variation of the net long wave radiation flux.

Dashed line for case A.
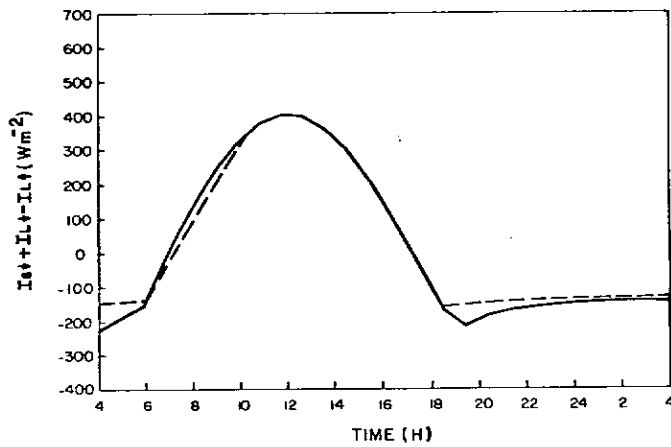
Full line for case B.

Fig. 4 - Diurnal variation of the net radiation flux.

Dashed line for case A.

Full line for case B.

Because the diurnal variations of the net radiation fluxes are similar in both cases, the diurnal cycles of the other characteristic PBL parameters are also similar.

5.2 - COMPARISONS BETWEEN CASE B AND C

In this section the influence of the humidity in the Kuo and Qian's parameterization is investigated. The relative humidity in case C was taken constant (80%) for all levels.

The diurnal variations of some PBL parameters for case B (dry air) and case C (including humidity) are presented for comparison.

The diurnal ground temperature variation, showed in Figure 5, is correctly simulated in both cases, in despite of some minor differences. The diurnal values of ground temperature in case C are higher than in case B due to the water vapor counterradiation effect. This can be explained analysing the diurnal net radiation flux showed in Figure 6.
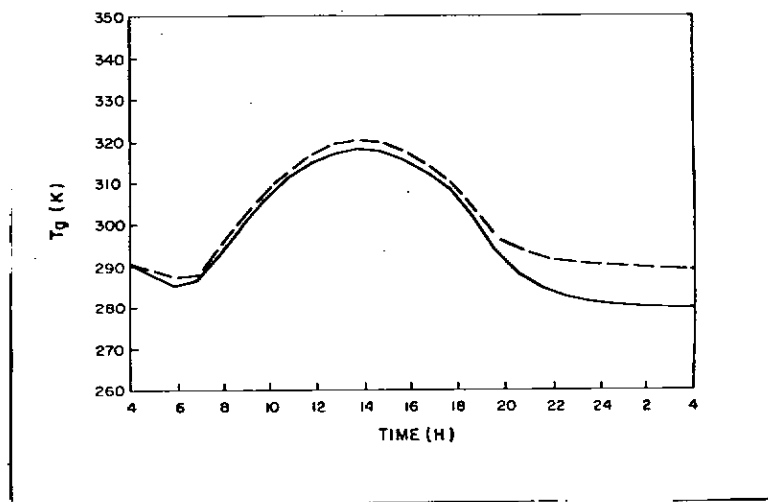
Fig. 5 - Diurnal ground temperature variation.
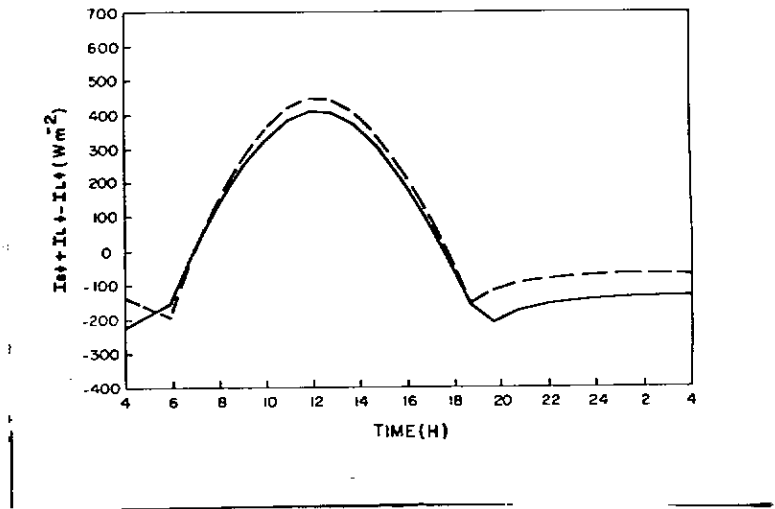
Dashed line for case C.
Full line for case B.

Fig. 6 - Diurnal net radiation flux variation.

Dashed line for case C.

Full line for case B.

During the day in spite of the short wave radiation
flux in case C, be less than in case B because the water vapor
absorption effect as seen in Figure 7, the amount of energy lost to
space is less than in case B due to water vapor counterradiation flux.
Thus, the net long wave radiation flux in case C is less than in case
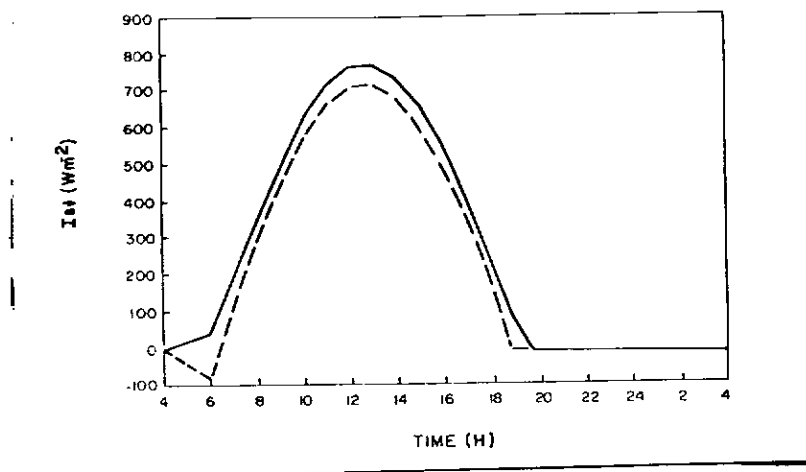B, as seen in Figure 8.

Fig. 7 - Diurnal solar radiation flux variation.

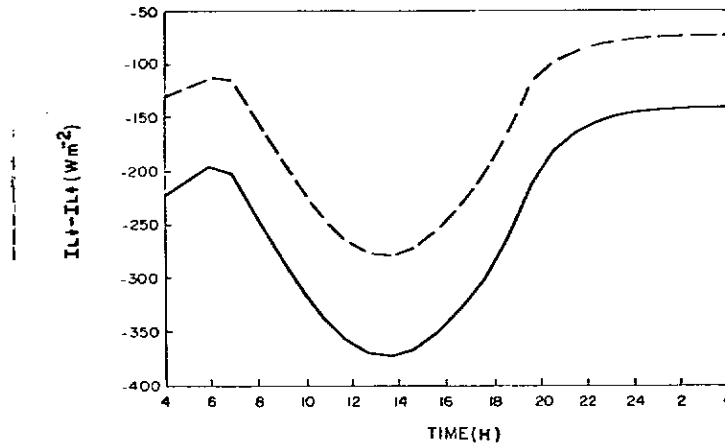Dashed line for case C.

Full line for case B.

Fig. 8 - Diurnal net long wave radiation flux variation.

Dashed line for case C.
Full line for case B.

Another important parameter that should be analysed is diurnal variation of the screen level potential temperature. Figure 9 shows again higher values of potential temperatures in case C. This fact is also related to the presence of water vapor as already explained in the previous analysis. Note that the values decrease quickly after 18:00h (local time) as the ground temperature becomes lower than the screen level potential temperature.

Figure 10 shows the diurnal variation of the sensible heat flux. During the day the values of H_o are higher in case C. This occurs because the values of T_* are smaller in case C (see Figure 11) implying in higher values of H_m in case C.

The values of H_c are also higher in case C because the values of θ_a are higher as already seen in Figure 9.. During the night the sensible heat flux is null in both cases because there is no convective flux and the mechanic flux is negligible since $T_a \sim T_g$, and therefore T_* is zero, as seen in Figure 11.
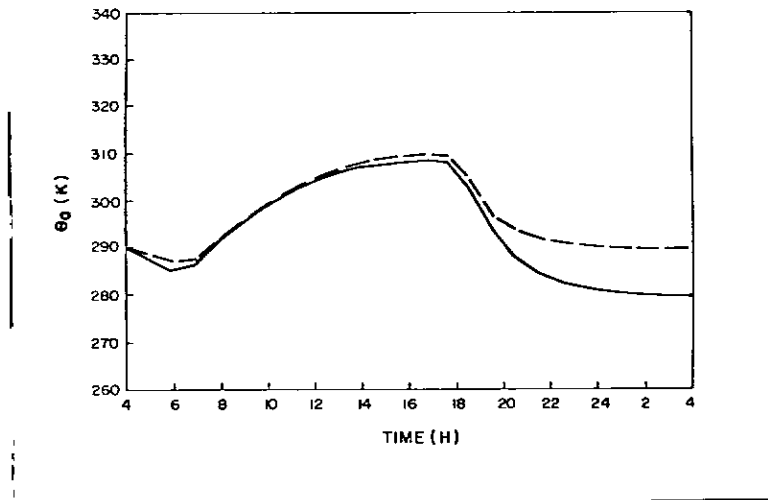
Fig. 9 - Diurnal screen level potential temperature variation.

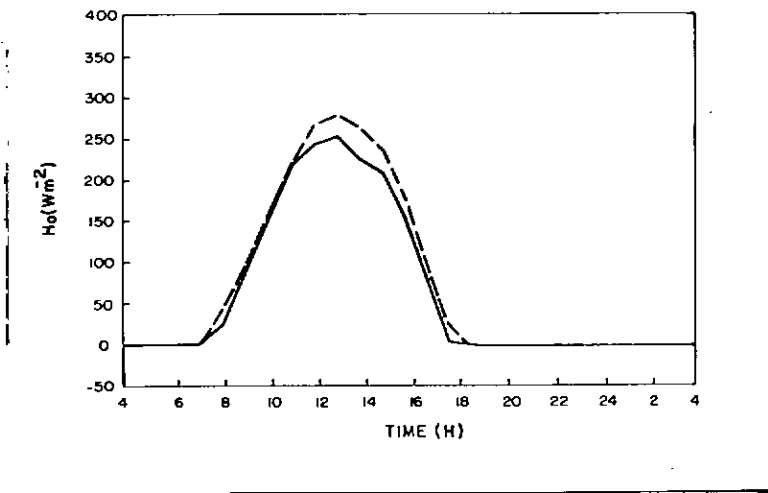Dashed line for case C.
Full line for case B.

Fig. 10 - Diurnal variation of the sensible heat flux.

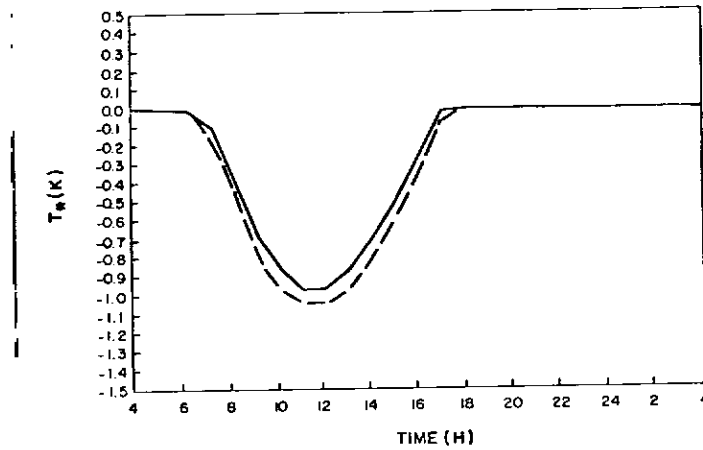Dashed line for case C.
Full line for case B.

Fig. 11 - Diurnal variation of the frictional temperature scale.

Dashed line for case C.

Full line for case B.

The behaviour of the friction velocity is showed in Figure 12. During the day the friction velocity is the same for both cases. In the early night it is zero for both cases, but probably because the presence of water vapor the values of u_* in case C begin to raise one hour before the case B.
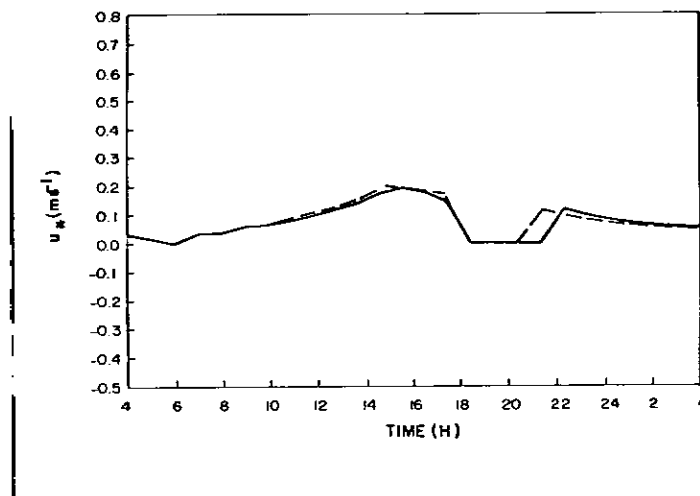

Fig. 12 - Diurnal variation of the friction velocity.

Dashed line for case C

Full line for case B.

Finally, the evaluation of the PBL height, and
vertical potential temperature profiles are showed in Figure .13.
The model succesfully simulated the diurnal development of the PBL
and the characteristic of the inversion. There are no significant
differences between θ profiles in both cases although the heights of
PBL are slightly higher in case C. Analyses made with the results
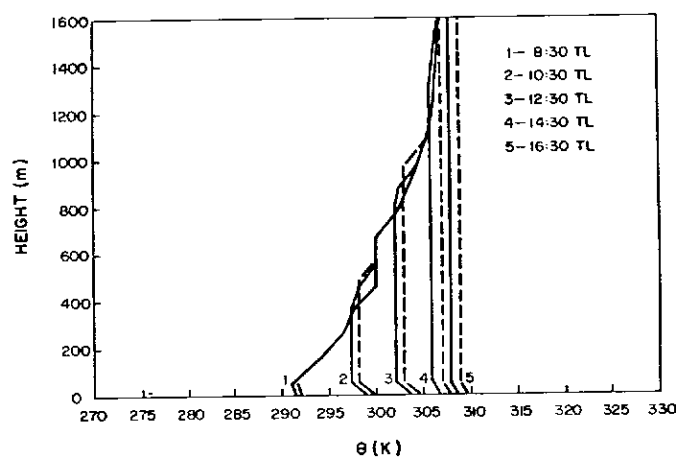obtained by the model seem to be in a good agreement with real data.

Fig. 13 - Potential temperature profiles.

Dashed lines for cases C.
Full lines for cases B.

6. CONCLUSIONS AND SUGGESTIONS

In the present study the model was developed for
simulations and not for predictions. The model gave a good simulation
of the diurnal behavior of several important parameters of the
planetary boundary layer in all cases studied. The case C, with more
physics than case A or B.presented more realistic results. The
developed model can be easily implemented in meso and large scale
models.

Further experiments and improvement can be made through inclusion of cumulus parameterization, and extension for two and three dimensions to produce more realistic results. Since this model can simulate diurnal variation of ground temperature, it can be used to support other frost prediction techniques. Other interesting experiment could be done taking different values of u_g and v_g.

The CPU time in a CDC 170/750 computer for the three cases was: 81.167S (case C), 80.992S (case B) and 6.2585S (case A). As the results of case A are similar to case B it is suggested that experiments considering dry air should be done using the Brunt's and Chang's parameterization to save CPU time.

REFERENCES

BLACKADAR, A.K. Modeling the nocturnal boundary layer. In: SYMPOSIUM ON ATMOSPHERIC TURBULENCE, DIFFUSION, AND AIR QUALITY, 3., North Carolina. 1976. *Reprints*. Raleigh, NC. American Meteorological Society, 1976, p. 46-49.

BUSINGER, J.A. Note on the critical Richardson number. *Quarterly Journal of the Royal Meteorological Society*, 95(sf):653-654, 1969.

—————— Turbulent transfer in the atmospheric surface layer. In: HAUGEN, D.A., ed. *Workshop on Meteorology*, Boston, MA. American Meteorological Society, 1973, p. 67-99.

BRUNT, D. *Physical and dynamical meteorology*. Cambridge, Cambridge University Press, 1952.

CHANG, S.W. An efficient parameterization of convective planetary boundary layer for use in a numerical model. In: CONFERENCE ON NUMERICAL WEATHER PREDICTION, 4., Silver Spring, Md, 1979. Preprints. Boston, MA. American Meteorological Society, 1979, p. 370-377.

DEARDORFF, J.W. The countergradient heat fluxes in the lower atmosphere and laboratory. *Journal of the Atmospheric Sciences*, 23(5):503-506, 1966.

FRANCHITO, S.H.; YAMAZAKI, Y. *A simplified model for boundary layer*. São José dos Campos, INPE, nov. 1982. (INPE-2588-PRE/236).

HINES, C.O. Generalizations of the Richardson criterion for the on set atmospheric turbulence. *Quarterly Journal of the Royal Meteorological Society*, 97(414):429-439, 1971.

HOFFERT, M.I.; STORCH, J. A scheme for computing surface fluxes from mean flow observations. *Boundary Layer Meteorology*, 17(3):429-442, 1979.

KONDRATYEV, K. Ya. *Radiation in the atmosphere.* New York, Academic Press, 1969.

KUO, H.L. Analytic infrared transmissivities of the atmosphere. *Beitrage Zur Physik der Atmosphäre,* 50(sf):331-349, 1977.

KUO, H.L.; QIAN, Y.F. Influence of the tibetian plateau on cumulative and diurnal changes of weather and climate in summer. *Monthly Weather Review,* 109(11):2337-2356, 1981.

LETTAU, H.H.; DAVIDSON, B. Exploring the atmosphere's first mile. In: GREAT PLAINS TURBULENCE FIELD PROGRAM. Proceeding. O'Neill, Nebraska - 1 Aug.. to 8 Sept. 1953. New York, Pergamon, 1957, p. 337-576.

PRIESTLEY, C.H.B. Turbulent transfer in the lower atmosphere. Chicago Press, 1965.

SMITH, F.B.; CARSON, D.J. Some thoughts on the specification of the boundary layer relevant to numerical modeling. *Boundary Layer Meteorology,* 12(3):307-330, 1977.

TAYLOR, G.I. Effect of variation in density on the stability of superposed streams of fluids. *Proceedings of the Royal Society of London; Serie A,* 132:449-523, 1931.